Journal of Applied Polymer Science

Preparation of a cellulose acetate/organic montmorillonite composite porous ultrafine fiber membrane for enzyme immobilization

Jinning Zhang,[1] Mingyu Song,[1] Xiaoyu Wang,[1] Jieru Wu,[1] Zhanping Yang,[2] Jianhua Cao,[2] Yun Chen,[2] Qufu Wei[1]

[1]Key Laboratory of Eco-Textiles (Ministry of Education), Jiangnan University, Wuxi 214122, Jiangsu, People's Republic of China
[2]Technical Center, Nantong Cellulose Fiber Company, Nantong 226008, Jiangsu, People's Republic of China
Correspondence to: Q. Wei (E-mail: qfwei@jiangnan.edu.cn)

ABSTRACT: Four types of fibrous membranes based on cellulose acetate (CA)—CA membranes with nonporous fibers, CA/organic montmorillonite (O-MMT) membranes with nonporous fibers, CA membranes with porous fibers, and CA/O-MMT membranes with porous fibers—were prepared by electrospinning, and then, they were used for enzyme immobilization. The surface morphologies of the composite fibrous membranes were investigated with scanning electron microscopy and transmission electron microscopy. The optimum pH was 3.5 for all of the immobilized enzymes, and the optimum temperature was 50 °C. Compared with the free enzyme, the immobilized enzyme showed better stability for pH and temperature changes. Moreover, the addition of O-MMT and the pores on the fibers improved the storage stability and the operational stability. Among the four kinds of fibrous membranes, the CA/O-MMT membranes with porous fibers showed the best stability for the immobilized enzymes. © 2016 Wiley Periodicals, Inc. J. Appl. Polym. Sci. **2016**, *133*, 43818.

KEYWORDS: adsorption; clay; fibers; membranes; porous materials

Received 28 December 2015; accepted 20 April 2016
DOI: 10.1002/app.43818

INTRODUCTION

Laccase, a copper-containing enzyme, can catalyze the oxidation of various substances.[1,2] Because of its good efficiency and low cost, it has been widely used in various applications, such as environmental bioremediation,[3] paper manufacturing,[4] food industry applications,[5] wood processing,[6] and textile industry applications.[7] However, the free enzyme cannot be recycled. Enzyme immobilization can make repeated use possible and improve the stability of the enzyme.[8]

Enzyme-immobilization technologies, including entrapment, adsorption, covalent binding, encapsulation, and self-immobilization, have been reported.[9] Among all of these methods, adsorption, which is relatively cheap and simple, may have a higher commercial potential.[10] Fibrous membranes with large surface areas, which have been recognized as excellent supports,[11] can fabricated by electrospinning, and enzymes can be adsorbed onto the membranes by ionic and/or other forces.

Cellulose acetate (CA), a derivative of cellulose, can be electrospun into ultrafine fibers. Because of its good thermal stability, chemical resistance, and biodegradability, CA has attracted a great deal of attention.[12] To improve the specific surface areas of ultrafine fibers, porous fibers have been widely studied. Celebioglu and Uyar[13] studied the morphology change of the porous CA fibers. Wang *et al.*[14] used porous fibrous membranes for air filtration. However, there has been no literature report on the use of CA membranes with porous fibers as a carrier of laccase. In addition, because of its excellent intercalation and swelling properties, good adsorption, and high affinity for several substances, montmorillonite (MMT) is also beneficial for laccase immobilization.[15] In addition, MMT is easily electrospun with different materials for various applications.[16]

In this study, ultrafine nonporous and porous CA fibers were produced by electrospinning. The membranes of nonporous CA fibers, porous CA fibers, nonporous CA/organic montmorillonite (O-MMT) fibers, and porous CA/O-MMT fibers were used as laccase carriers. Finally, the immobilized enzyme properties, including the optimum pH, optimum temperature, operational stability, and storage stability, were investigated. Among the four kinds of fibrous membranes, the CA/O-MMT membranes with porous fibers showed the best stability for the immobilized enzymes.

EXPERIMENTAL

Materials

Laccase from *Trametes versicolor* (activity $\geq$ 0.5 U/mg) was obtained from Sigma–Aldrich. 2,2′-Azino-*bis*-(3-ethylbenzothiazoline-

Table I. Solutions for the Electrospinning of the CA Ultrafine Fibrous Membranes

Solution	CA solution concentration (wt %)	O-MMT concentration (wt %)	DCM/DMAC (v/v)	DCM/acetone (v/v)
Nonporous CA	16	—	—	3/2
Nonporous CA/O-MMT	16	0.05	—	3/2
Porous CA	4	—	4/1	—
Porous CA/O-MMT	4	0.05	4/1	—

6-sulgonic acid) diammonium salt (ABTS) was provided by Sigma–Aldrich. CA (Iv = 1.45, Wn = 8.4×10^4) was obtained from Nantong Cellulose Fibers Co., Ltd. (Nantong, China). O-MMT (cation-exchange capacity = 97 mequiv/100 g) was purchased from Zhejiang Fenghong Clay Chemical Co., Ltd. (Zhejiang, China). Dichloromethane (DCM), *N,N*-dimethylacetamide (DMAC), and acetone were all purchased from Sinopharm Chemical Reagent Co., Ltd. All of the chemicals were used without further purification.

Preparation of the CA Ultrafine Fibrous Membranes

Four kinds of CA ultrafine fibrous membranes (CA membranes with nonporous fibers, CA/O-MMT membranes with nonporous fibers, CA membranes with porous fibers, and CA/O-MMT membranes with porous fibers) were prepared by electrospinning. CA solutions were prepared by the dissolution of CA in a mixture of DCM and DMAC (3/2 v/v) or a mixture of DCM and acetone (4/1 v/v) by stirring for 6 h until a homogeneous solution was obtained. Although the O-MMT was put into the CA solutions, the CA/O-MMT solutions were obtained. All of the CA solutions were prepared as listed in Table I.

Then, the solution was loaded into a syringe and ejected through a metal needle. A positive voltage of 18 kV was applied to the needle tip through a high-voltage supply (DW-P503-1ACF0, Tianjin Dongwen High Voltage Co., China). The feed rate operated by a syringe pump (JZB-1800D, Changsha Jianyuan Medical Technology Co., Ltd.) was set as 1 mL/h. The working distance was 15 cm. The CA ultrafine membranes were deposited on a grounded metallic rotating roller at a rate of 8 mL/h.

Immobilization of Laccase on CA Ultrafine Fibrous Membranes

The laccase was dissolved in a HAc–NaAc (pH = 4.5) solution at a concentration of 1 g/L. The mixture was stirred by magnetic stirring for 30 min in an ice bath.

Then, the four kinds of prepared CA ultrafine fibrous membranes were used as the enzyme carriers. They (at 50 mg accurately weighted) were put into the centrifuge tubes. Then, a 5-mL enzyme solution was placed into the centrifuge tubes, too. The centrifuge tubes with membranes and enzyme solution were put into refrigerator for 12 h at 4 °C. Finally, the fibrous membranes were taken out and washed several times by an HAc–NaAc solution until no laccase could be washed into the HAc–NaAc solution.

Activity Assays of Free and Immobilized Laccase

The ABTS was used as the substrate to assay the activity of free and immobilized laccase. The activities of the free enzyme and immobilized laccase were determined at 30 °C. For the free enzyme, a 2.8-mL HAc–NaAc solution and a 0.1-mL enzyme solution were added to the centrifuge tube. After 0.1 mL of ABTS (15 m*M*, dissolved in HAc–NaAc solution) was put into the centrifuge tube for 2.5 min at 30 °C with constant shaking. The absorbance of the solution was measured with ultraviolet–visible spectrophotometry at a wavelength of 420 nm. In the case of the immobilized enzyme, the CA ultrafine fibrous membranes were taken out after the immobilization process. Then, the 50-mg membranes were immersed into a 2.8-mL HAc–NaAc solution. The following steps were the same as those used for the free laccase:

$$\text{Unit activity} = 1000AV/(t\varepsilon M_0) \quad (1)$$

where A is the absorbance at reaction time t, V is the reaction solution volume, ε is the molar extinction coefficient for the oxidation of ABTS at a wavelength of 420 nm, and M_0 is the laccase mass.

Characterization

Scanning electron microscopy (SEM; S-4800, Hitachi, Tokyo, Japan) was used to observe the morphologies of different electrospun nanofibrous membranes and to examine the effect of the laccase immobilization on the surface morphologies. The fibrous membranes were collected on an aluminum SEM disk and then coated with 5 nm of gold. Transmission electron microscopy (TEM; JEOL/JEM-2100, Japan) was used to analyze the distribution of the O-MMT in the polymer fibers. A copper grid was used to collect the polymer jet in the place of the collector during the electrospinning process for a few seconds, and was then put in an oven at 60 °C for 2 h. Ultraviolet–visible spectrophotometry (UV-2201, Japan) was used to evaluate the properties of the immobilized enzyme.

RESULTS AND DISCUSSION

Formation Mechanism of the Porous Fibers

A typical SEM image of the porous CA fibers fabricated from a 4 wt % CA solution in DCM/acetone is shown in Figure 1. Figure 1(a) shows that the diameter of fibers looked relatively even, and the pores were formed on the fiber surface. Figure 1(b) reveals the porous fibers at a higher magnification. The pores sizes appeared different, and all of them formed different shapes. It was clear that the pores were deformed along the fiber axis; this may have been caused by the electrostatic draft during the process of electrospinning.

Figure 2 shows the mechanism of the formation of ultrafine porous CA fibers during electrospinning.[14,17] The initial

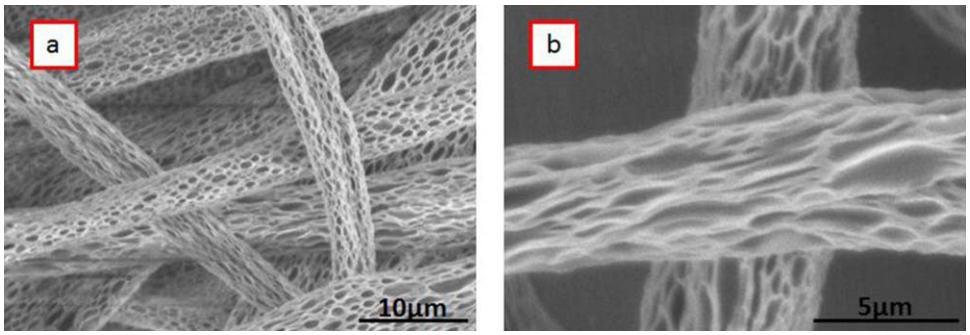

Figure 1. SEM images of the porous fibers electrospun from a 4 wt % CA solution in DCM/acetone at (a) lower and (b) higher magnifications. [Color figure can be viewed in the online issue, which is available at wileyonlinelibrary.com.]

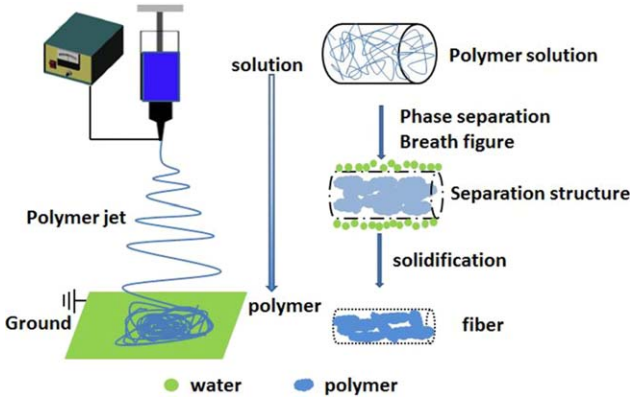

Figure 2. Schematic mechanism of the process of ultrafine porous CA fiber formation during electrospinning. [Color figure can be viewed in the online issue, which is available at wileyonlinelibrary.com.]

polymer solution was homogeneous and consisted of the CA polymer and solvent. The homogeneous polymer solution was ejected into the air environment during electrospinning. Because of the low boiling point of the solvent, the solvent on the jet surface evaporated rapidly into the air environment, and at the same time, the solvent within the jet spread out. The temperature of the solution jet rapidly decreased; this caused the jet to be thermodynamically unstable. The separation structure formed in a short time. The jet would divide into a polymer-rich phase and polymer-lean phase.[18,19] In addition, the breath figure also made some influence.[20] Because of the low temperature of the jet, the water vapor in the air environment condensed to water droplets on the jet surface. Because of the insolubility of the CA polymer in the water droplet, the membrane formed on the surface of the jet when the solution met the water droplets; this also prevented blending between the water droplets. After the elongation and volatilization, the polymer-lean phase and water droplets formed the pores of the fibers, and the polymer-rich phase formed the matrix of the fibers.

Structures of CA Membranes with Nonporous Fibers and Porous Fibers

The solution properties were an important parameter affecting the morphology of the fibers. The characterization of the four kinds of solutions is shown in Table II. The viscosity and conductivity of the 16% solution were much higher than those of the 4% solution. The addition of MMT increased the conductivity of the solution. SEM images of the four kinds of CA ultrafine fibrous membranes (CA membranes with nonporous fibers, CA/O-MMT membranes with nonporous fibers, CA membranes with porous fibers, and CA/O-MMT membranes with porous fibers) are shown in Figure 3. The four kinds of CA ultrafine fibrous membranes had different morphologies. All of the nanofibers were randomly distributed to form the membranes. Compared with the porous fibers, the nonporous fibers had much thinner diameters. As shown in Figure 3(a), the average diameter of the electrospun CA fibers was about 740 nm. After O-MMT added, the average diameter of the electrospun CA/O-MMT fibers decreased, but the diameter of the fibers was not very uniform, and some beads were observed on the fiber, as presented in Figure 3(b). As for the porous fibers, the diameter of the fibers looked relatively uniform. The pores were obvious, as shown in Figure 3(c,d).

The TEM images of the four kinds of CA fibers are displayed in Figure 4 and represent the distribution of O-MMT in the polymer fibers. The nonporous CA fibers without O-MMT had a coincident contrast and uniform structure, as presented in

Table II. Characterization of the Four Kinds of Solutions with the Corresponding CA Fibers

Solution	Viscosity (mPa s)	Conductivity (μs/cm)	Average fiber diameter (μm)	Fiber diameter range (μm)
Nonporous CA	1820.0	3.18	0.71	0.34–0.91
Nonporous CA/O-MMT	1900.0	5.99	0.57	0.27–1.32
Porous CA	107.5	0.46	3.21	2.43–4.26
Porous CA/O-MMT	111.7	0.92	3.09	2.09–4.47

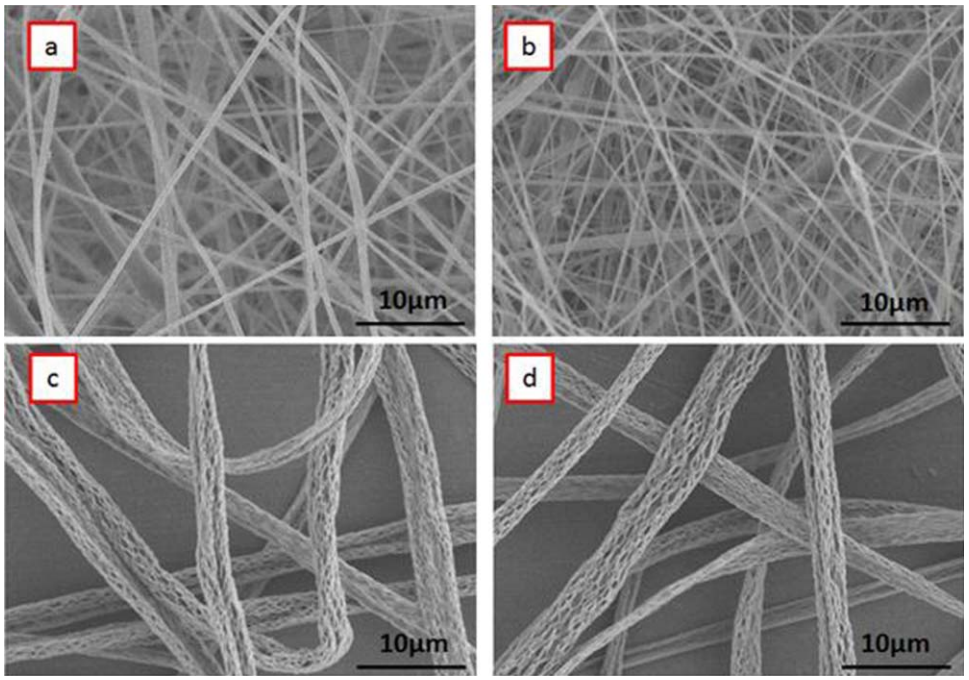

Figure 3. SEM of the (a) CA membranes with nonporous fibers, (b) CA/O-MMT membranes with nonporous fibers, (c) CA membranes with porous fibers, and (d) CA/O-MMT membranes with porous fibers. [Color figure can be viewed in the online issue, which is available at wileyonlinelibrary.com.]

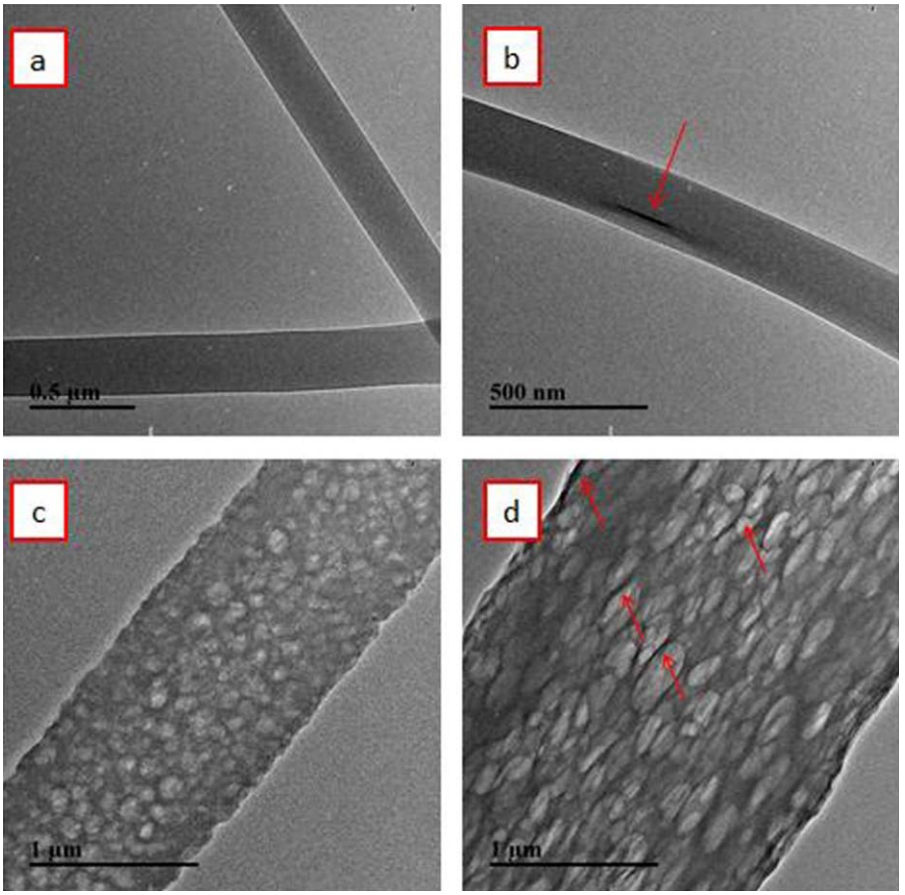

Figure 4. TEM of the (a) nonporous CA fibers, (b) nonporous CA/O-MMT fibers, (c) porous CA fibers, and (d) porous CA/O-MMT fibers. [Color figure can be viewed in the online issue, which is available at wileyonlinelibrary.com.]

Figure 4(a). For the nonporous CA/O-MMT fibers, the existence of the layered structure were found along the fiber axial alignment; this demonstrated that the inclusion of O-MMT in the fiber matrix, as shown in Figure 4(b). Compared with the nonporous fibers, porous structures were clearly observed on the porous CA fibers. For the porous CA/O-MMT composite fibers, some layer structures were also found within the polymer fiber, and their distributions were more uniform than those existing in the nonporous CA/O-MMT fibers.

The N_2 adsorption–desorption isotherms of the four kinds of membranes are shown in Figure 5(a). We observed that all of the samples were type IV from Brunauer–Deming–Deming–Teller classification; this indicated that the membranes possessed the features of open mesopores (2–50-μm pore width) and macropores (>50-μm pore width). The Brunauer–Emmett–Teller (BET) surface area is shown in the table inset of Figure 5(a).

The pore size distribution curves of the different membranes are shown in Figure 5(b). It was noteworthy that both of the membranes with nonporous fibers showed a pore size distribution in the range 2.0–3.0 μm; this confirmed that the membranes possessed a relatively narrow pore distribution. For membranes with porous fibers, the mean flow pore sizes of the CA membranes and CA/MMT membranes were 8.4767 and 10.0993 μm, respectively, because of the larger fiber diameters.

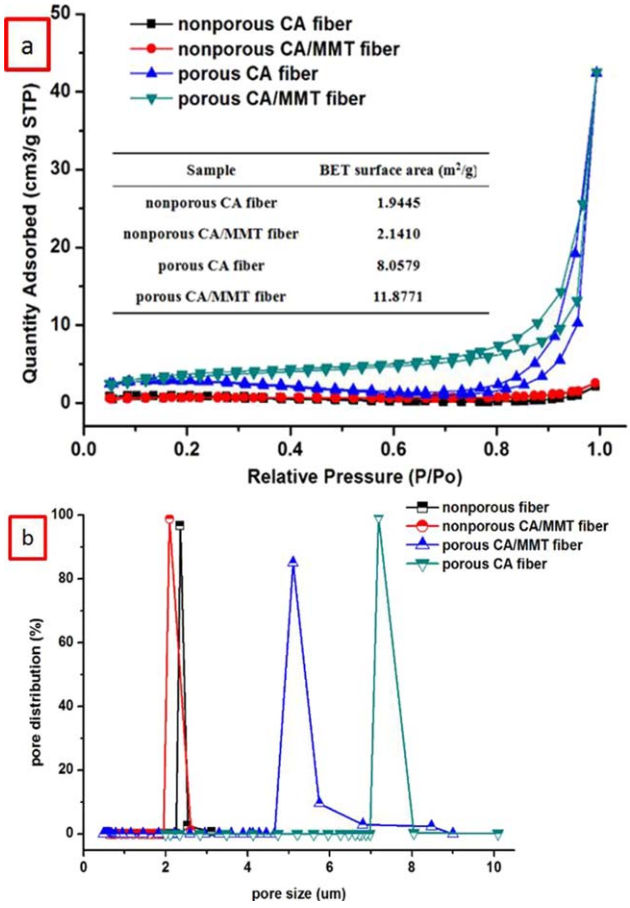

Figure 5. (a) N_2 adsorption–desorption isotherms of the four kinds of membranes (the inset shows the BET surface areas of the membranes) and (b) pore size distribution curves of different membranes. [Color figure can be viewed in the online issue, which is available at wileyonlinelibrary.com.]

Structures of the Electrospun Membranes after Enzyme Immobilization

The SEM images of the four kinds of CA membranes after enzyme immobilization are presented in Figure 6. Because of the swelling behavior, the four kinds of CA membranes after enzyme immobilization showed increased fiber diameters. In particular for porous fibers, the enzyme immobilization significantly altered the fiber morphologies. Figure 6(c,d) reveals that the fibers became flat after enzyme immobilization; this was because of the pressure of water and atmosphere during the enzyme immobilization and the drying process. The size of the pores on the porous fiber surface decreased; there might have been two reasons: one was the collapse of the fibers, and the others were enzyme-aggregated on the surface of the porous fibers. We also found that the pore size of the porous CA/O-MMT fibers in Figure 6(d) decreased more dramatically in comparison with those fiber in Figure 6(c); this was caused by the strong adsorption ability of O-MMT.

Properties of the Immobilized Enzyme

Optimum Temperature. To determine the effect of the temperature on enzyme immobilization, the relative enzyme activity was measured with free and immobilized laccase on the four kinds of CA fibers at different temperatures. As shown in Figure 7, the maximum enzyme activity observed was defined as 100%. As shown in the following equation[21]:

$$R_r = (A/A_{max}) \times 100\% \quad (2)$$

where R_r is the relative activity of the free and immobilized laccase, A is the absorbance measured in a certain reaction time, and A_{max} is the maximum absorbance measured under different reaction conditions.

Figure 7 shows that the temperature had a great effect on the stability of the free and immobilized laccase. We observed that the relative activities of the free and immobilized laccase all increased with increasing environmental temperature; after the optimum temperature was achieved, the relative activities all decreased with increasing environmental temperature. This was because of the inactivation of the enzyme at high temperature. The optimum temperatures of the free and immobilized laccase were all at about 50 °C. Compared with free enzyme, the immobilized enzyme had better tolerance for the change in temperature; this was in accordance with other reports.[22] Among all of the immobilized enzymes, the sample with the porous CA/O-MMT fibers as the carrier showed the best temperature stability and had the broadest range temperature profile. The immobilized enzymes with nonporous CA as a carrier showed a trend close to that of the free enzyme, whereas the immobilized enzymes with nonporous CA/O-MMT and porous CA as carriers had relatively better temperature stability than the free enzyme.

Optimum pH. The pH stabilities of the free and immobilized laccase on the four kinds of CA fibers are shown in Figure 8.

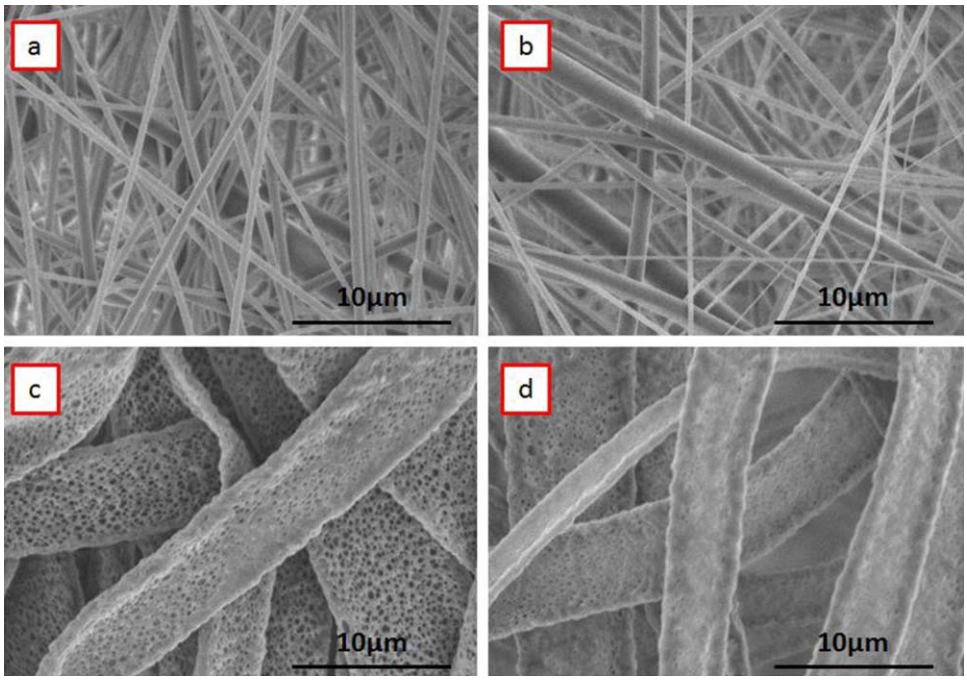

Figure 6. SEM images of the different membranes after enzyme immobilization: (a) CA membranes with nonporous fibers, (b) CA/O-MMT membranes with nonporous fibers, (c) CA membranes with porous fibers, and (d) CA/O-MMT membranes with porous fibers. [Color figure can be viewed in the online issue, which is available at wileyonlinelibrary.com.]

We observed that the optimum pHs of all of the free and immobilized enzymes were about 3.5 in the experiment. The immobilized enzyme showed a broader tolerance for the change in pH than the free enzyme; this was also observed in other studies.[23] Changes in the environment pH values made the difference in the binding and catalysis ability between the enzyme and substrate, and in the end, the dissociation degree of the substrate was affected.[24] In addition, the porous CA/O-MMT fibers immobilized with the four kinds of immobilized enzymes showed a similar trend as the free enzyme but the best pH value range. In addition, the nonporous CA/O-MMT fibers, porous CA fibers, and nonporous CA fibers also showed a trend similar to that of the free enzyme, but the relative activity was lower than that of the porous CA/O-MMT fibers immobilized with enzyme.

Storage Stability. The storage stabilities of the free and immobilized laccase on the four kinds of CA fibers were also studied, and the results are shown in Figure 9. After 20 days, the immobilized enzymes all maintained relative activities of more than 50%; this was much better than the free enzyme. Among the four kinds of enzyme-immobilized fibers, the porous CA/O-MMT fibers and porous CA fibers showed the best relative activity at the beginning of the 12 days, and later, the porous

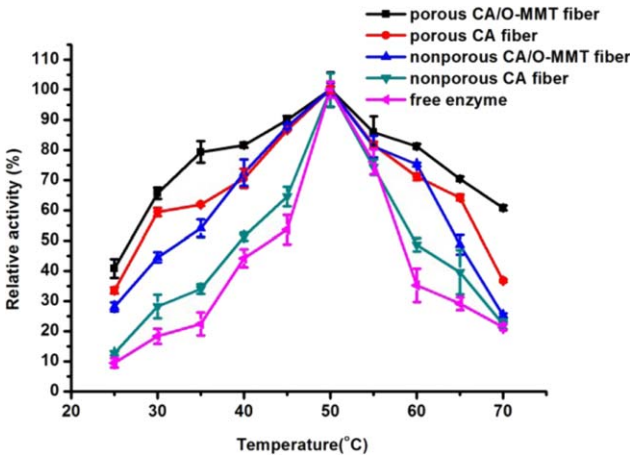

Figure 7. Effect of the temperature on the activity of free and immobilized laccase on the four kinds of CA fibers. [Color figure can be viewed in the online issue, which is available at wileyonlinelibrary.com.]

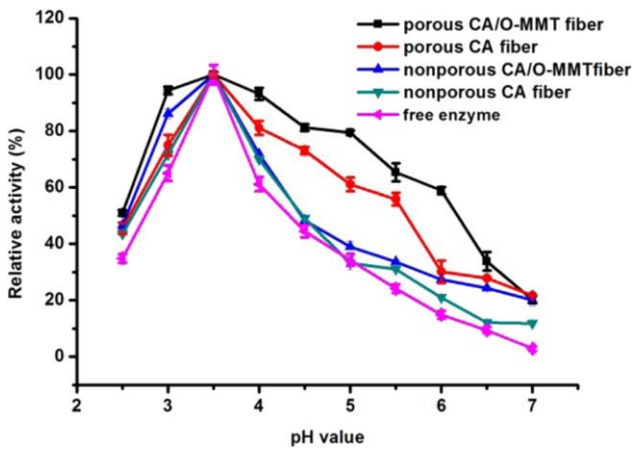

Figure 8. Effect of the pH on the activity of the free and immobilized laccase on the four kinds of CA fibers. [Color figure can be viewed in the online issue, which is available at wileyonlinelibrary.com.]

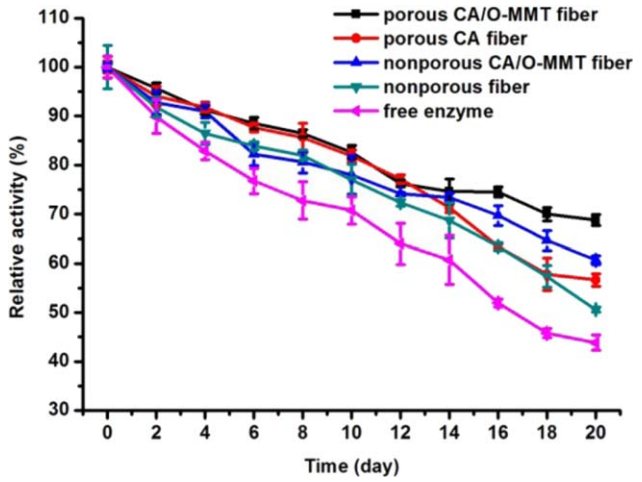

Figure 9. Storage stability of the free and immobilized laccase on the four kinds of CA fibers. [Color figure can be viewed in the online issue, which is available at wileyonlinelibrary.com.]

CA/O-MMT fibers showed a relatively higher storage stability than the others.

Operational Stability. The operational stability of the immobilized laccase is presented in Figure 10. To reduce the cost of the product, it was important to improve the operational stability. Because of the larger specific surface area of the porous fibers and the better adsorptive properties of O-MMT, the porous CA/O-MMT fibers had the best operational stability among them. After seven repeated recycles, the relative activity of the immobilized enzyme on the porous CA/O-MMT fibers remained at around 50%. Compared with the nonporous CA fibers, the porous CA and nonporous CA/O-MMT fibers showed better relative activities; the results indicate that the porous structure and the existence of the O-MMT were beneficial for maintaining the enzyme activity.

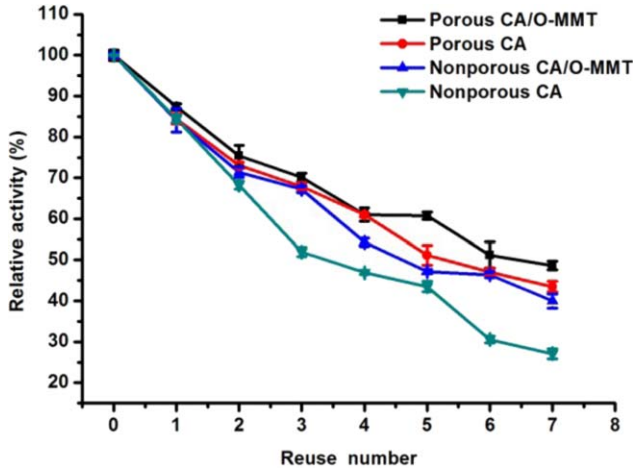

Figure 10. Operational stability of the immobilized laccase on the four kinds of CA fibers. [Color figure can be viewed in the online issue, which is available at wileyonlinelibrary.com.]

CONCLUSIONS

In this study, four kinds of CA fibrous membranes—CA membranes with nonporous fibers, CA/O-MMT membranes with nonporous fibers, CA membranes with porous fibers, and CA/O-MMT membranes with porous fibers—with different morphologies were prepared successfully by electrospinning. They were used as carries for enzyme immobilization. The results show that the existence of O-MMT and the pores on the fibers contributed to the enzyme activity. In addition, the porous CA/O-MMT membranes could be used at least seven times and could still maintain more than 50% of its relative activity. The results of this study imply that the CA/O-MMT membrane with porous fibers could be a good candidate for enzyme immobilization.

ACKNOWLEDGMENTS

This work was financially supported by the Six Talent Peaks Project in Jiangsu Province (contract grant number 2014-XCL001), the Industry–Academia–Research Joint Innovation Fund of Jiangsu Province (contract grant number BY2014023-06), the Fundamental Research Funds for the Central Universities (contract grant number JUSRP51621A), and the Innovation Program for Graduate Education in Jiangsu Province (contract grant number KYLX15_1183).

REFERENCES

1. Galhaup, C.; Goller, S.; Peterbauer, C. K.; Strauss, J.; Halrtich, D. *Microbiology* **2002**, *148*, 2159.
2. Wang, Q. Q.; Cui, J.; Li, G. H.; Zhang, J. N.; Huang, F. L.; Wei, Q. F. *Polymer* **2014**, *6*, 2357.
3. Ashrafi, S. D.; Rezaei, S.; Forootanfar, H.; Mahvi, A. H.; Faramarzi, M. A. *Int. Biodeterior. Biodegrad.* **2013**, *85*, 173.
4. Flory, A. R.; Requesens, D. V.; Devaiah, S. P.; Teoh, K. T.; Mansfield, S. D.; Hood, E. E. *BMC Biotechnol.* **2013**, *13*, 28.
5. Dhillon, G. S.; Kaur, S.; Brar, S. K.; Verma, M. *J. Agric. Food Chem.* **2012**, *60*, 7895.
6. Fackler, K.; Kuncinger, T.; Ters, T.; Srebotnik, E. *Holzforschung* **2008**, *62*, 223.
7. Basto, C.; Tzanov, T.; Cavaco-Paulo, A. *Ultrason. Sonochem.* **2007**, *14*, 350.
8. Lu, L.; Zhao, M.; Wang, Y. *World J. Microbiol. Biotechnol.* **2007**, *23*, 159.
9. Sheldon, R. A.; van Pelt, S. *Chem. Soc. Rev.* **2013**, *42*, 6223.
10. Bayramoglu, G.; Arica, M. Y. *Mater. Sci. Eng. C* **2009**, *29*, 1990.
11. Wang, Z. G.; Wan, L. S.; Liu, Z. M.; Huang, X. J.; Xu, Z. K. *J. Mol. Catal. B* **2009**, *56*, 189.
12. Baek, W. I.; Pant, H. R.; Nam, K. T.; Nirmala, R.; Oh, H. J.; Kim, I.; Kim, H. Y. *Carbohydr. Res.* **2011**, *346*, 1956.
13. Celebioglu, A.; Uyar, T. *Mater. Lett.* **2011**, *65*, 2291.
14. Wang, Z.; Zhao, C. C.; Pan, Z. J. *J. Colloid Interfaces Sci.* **2015**, *441*, 121.

15. Bhattacharyya, K. G.; Sen Gupta, S. *Adv. Colloid Interfaces* **2008**, *140*, 114.
16. Cai, Y. B.; Li, Q.; Wei, Q. F.; Wu, Y. B.; Song, L.; Hu, Y. *J. Mater. Sci.* **2008**, *43*, 6132.
17. Qi, Z. H.; Yu, H.; Chen, Y. M.; Zhu, M. F. *Mater. Lett.* **2009**, *63*, 415.
18. Megelski, S.; Stephens, J. S.; Chase, D. B.; Rabolt, J. F. *Macromolecules* **2002**, *35*, 8456.
19. Dayal, P.; Liu, J.; Kumar, S.; Kyu, T. *Macromolecules* **2007**, *40*, 7689.
20. Luo, C. J.; Nangrejo, M.; Edirisinghe, M. *Polymer* **2010**, *51*, 1654.
21. Zhang, P.; Wang, Q. Q.; Zhang, J. N.; Li, G. H.; Wei, Q. F. *Fiber. Polym.* **2014**, *15*, 30.
22. Wang, Q. Q.; Cui, J.; Li, G. H.; Zhang, J. N.; Huang, F. L.; Wei, Q. F. *Polymer* **2014**, *6*, 2357.
23. Bayramoglu, G.; Yilmaz, M.; Senel, A. U.; Arica, M. Y. *Biochem. Eng. J.* **2008**, *40*, 262.
24. Wang, Q. Q.; Peng, L.; Du, Y. Z.; Xu, J.; Cai, Y. B.; Feng, Q.; Huang, F. L.; Wei, Q. F. *J. Porous Mater.* **2013**, *20*, 457.